

Substructure in molecular outflow bullets from protostars.

Blázquez-Calero, G.¹, Osorio M.¹, Anglada G.¹, Gómez J.F.¹, Diaz-Rodriguez A.K.², and Fuller G.^{1,2,3}

¹ Instituto de Astrofísica de Andalucía, CSIC, Glorieta de la Astronomía s/n, 18008 Granada, Spain

² UK ALMA Regional Centre Node, Jodrell Bank Centre for Astrophysics, Department of Physics and Astronomy, The University of Manchester, Oxford Road, Manchester M13 9PL, UK

³ I. Physikalisches Institut, University of Cologne, Zùlpicher Str. 77, D-50937 Köln, Germany

Abstract

Some protostellar molecular outflows are associated with the so-called extremely high velocity molecular bullets, discrete clumps of gas ejected from the close environment of the protostar, travelling at velocities of >100 km/s. We carried out ALMA observations that resolve the morphology and kinematics of one of these molecular bullets. We present model results that account for the main observed features of the source.

1 Introduction

Outflows are an ubiquitous ingredient of the star formation process. Moreover, they are not a mere by-product of the protostar evolution, but they play an important role in the assembly of stars, can alter the properties of the protoplanetary disks and, consequently, they might be able to have an impact also on the planet formation process [12]. Outflows from young stellar objects usually present two different components. A highly-collimated and partially ionized component (the jet), which is traveling at extremely high velocities (~ 100 km/s), and a fairly collimated (and usually bipolar) component (the molecular outflow) with velocities of the order of 10 km/s. Jets are originated from the proximity of the star (likely from its accretion disk) and frequently observed at optical, infrared and radio wavelengths [7, 2, 21]. Jets are thought to be powerful enough to entrain ambient gas and produce the usually more massive molecular outflows ubiquitously observed in low-excitation transitions of CO and other molecular species at mm wavelengths [22, 16, 5, 18].

Nonetheless, for some young sources, the outflow also has a low excitation molecular component traveling at extremely high velocities of ~ 100 km/s. In these cases, we see that this

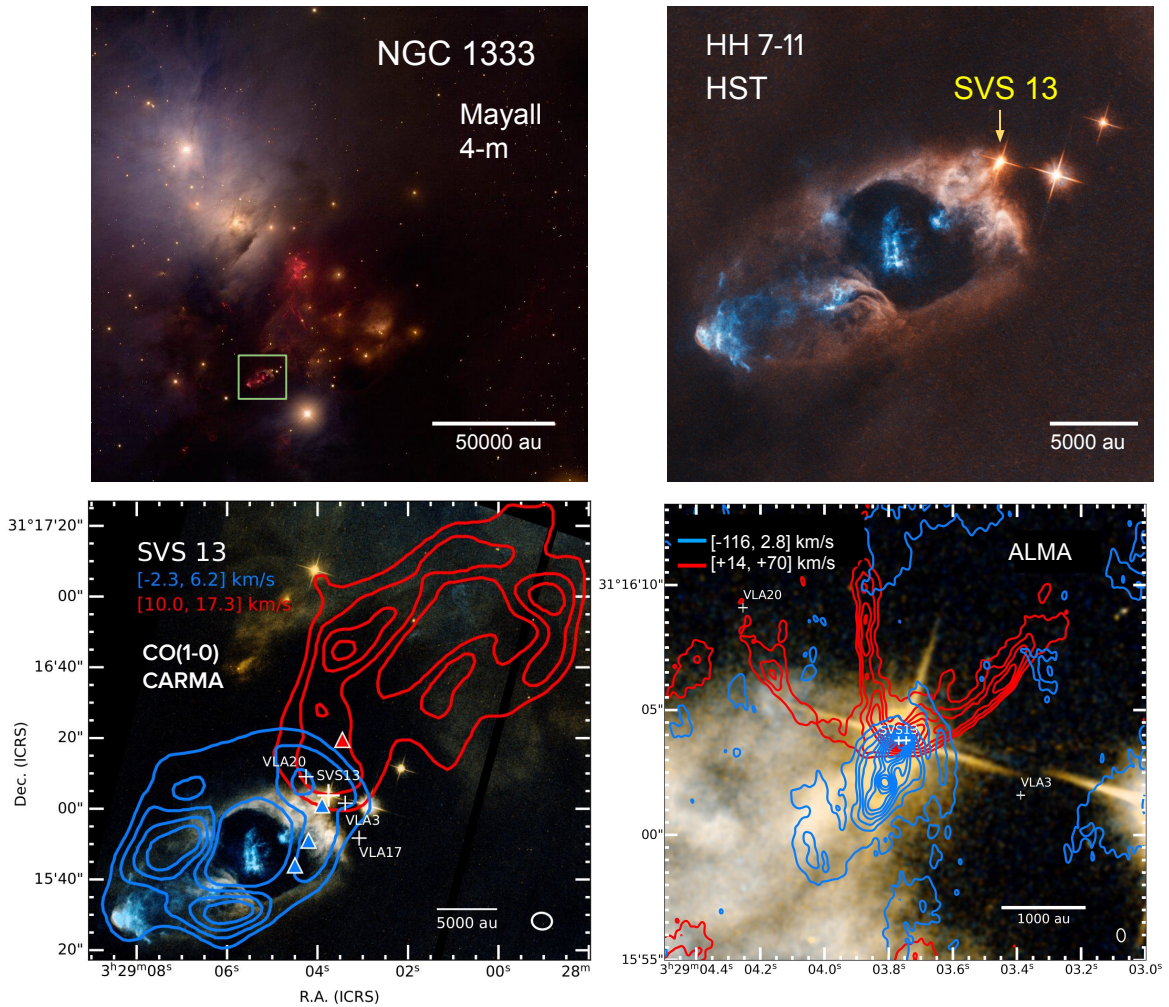


Figure 1: Top left: Optical (B, V, I, H α) image of the NGC 1333 star-forming region obtained with the Mayall 4-m telescope at Kitt Peak (credits: T.A. Rector/University of Alaska Anchorage, H. Schweiker/WIYN and NOIRLab/NSF/AURA). Top right: HST image (F606W filter) showing a close-up of the HH7-11 objects (from the Hubble Legacy Archive). Bottom left: CARMA CO(1-0) map of the blue-shifted and red-shifted lobes of the large-scale bipolar molecular outflow [20, 24], overlaid on the HST image. The triangles mark the location of the molecular bullets [6, 9]. Bottom right: ALMA CO(3-2) map (with a resolution of $0.520'' \times 0.324''$) of the blue-shifted and red-shifted integrated emission in a region close to the SVS 13 protostars. The image shows the arc-shaped walls of the outflow lobes, as well as the blue-shifted bullet closest to SVS 13 [8]. All velocities are with respect to the LSR. The systemic LSR velocity is $\sim +8.5$ km/s [11].

component appears not as a continuous jet but as a collection of roughly aligned discrete clumps called molecular bullets [3]. The observed bullets present typical separations corresponding

to time intervals of ~ 50 to ~ 1000 yr, and their masses are about $10^{-4} M_{\odot}$ (several orders of magnitude smaller than the masses of standard molecular outflows) [13, 19, 17, 23, 14, 28, 25].

Although several interpretations have been proposed for the extremely high velocity bullets [3, 4, 27], their true nature remains unclear. We obtained high angular and spectral resolution ALMA observations of one of these bullets associated to SVS 13 showing its substructure that can help to understand its nature [8].

2 The SVS13 outflow

Figure 1 shows an overview of the NGC 1333 region and the outflows associated with the SVS 13 at optical and millimeter wavelengths. Figure 2 shows our ALMA images of the molecular bullet closest to SVS 13.

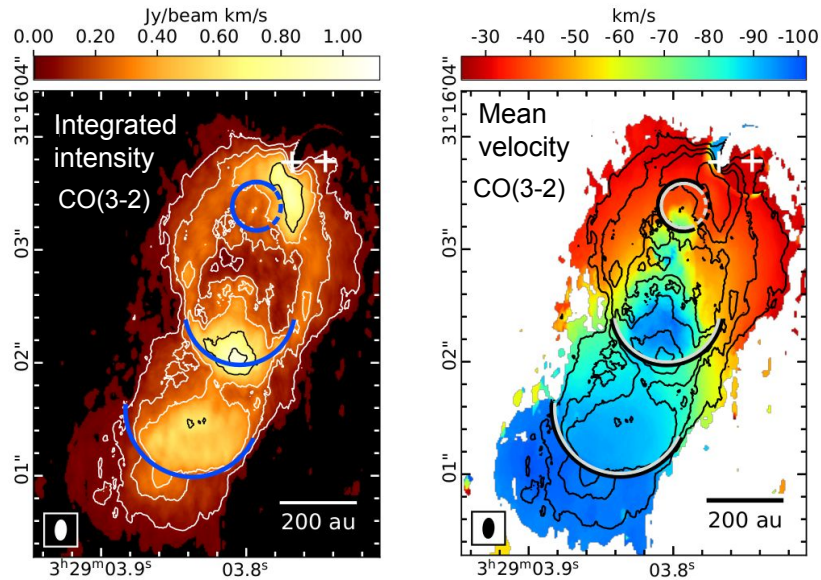


Figure 2: Left: Image of the velocity-integrated intensity (zeroth-order moment) of the molecular bullet closest to SVS 13, obtained from ALMA CO($J=3-2$) observations [8]. Right: Image of the mean velocity field (first-order moment), in color scale, overlaid on the integrated intensity (in contours). The velocities are line-of-sight velocities relative to the systemic velocity of the ambient cloud ($+8.5$ km/s; [11]). A clear global velocity gradient is seen along the major axis of the bullet. The images have been corrected by the decrease in sensitivity due to the primary beam response. The positions of the two protostars of the SVS 13 binary [1], near the top right corner of the images, are indicated by plus signs. The H₂ arcuate features imaged by [15] are plotted as arcs. The synthesized beam ($0.163'' \times 0.084''$, PA = 4.2°) is plotted as an ellipse in the bottom left corner of the images.

NSC and ASIAA (Taiwan) and KASI (Republic of Korea), in cooperation with the Republic of Chile. The Joint ALMA Observatory is operated by ESO, AUI/NRAO and NAOJ. This publication use images based on observations made with the NASA/ESA Hubble Space Telescope, and obtained from the Hubble Legacy Archive, which is a collaboration between the Space Telescope Science Institute (STScI/NASA), the Space Telescope European Coordinating Facility (ST-ECF/ESA) and the Canadian Astronomy Data Centre (CADAC/NRC/CSA).

References

- [1] Anglada, G., Rodríguez, L. F., Torrelles J. M. 2000, *ApJL*, 542, L123.
- [2] Anglada, G., Rodríguez, L. F., Carrasco-González C. 2018, *A&ARv*, 26, 3.
- [3] Bachiller, R., Cernicharo, J., Martín-Pintado, J., Tafalla, M., Lazareff, B. 1990, *A&A*, 231, 174
- [4] Bachiller, R., Martín-Pintado, J., Fuente, A. 1991, *A&A*, 243, L21
- [5] Bachiller, R. 1996, *ARA&A*, 34, 111.
- [6] Bachiller, R., Gueth F., Guilloteau S., Tafalla M., Dutrey A. 2000, *A&A*, 362, L33
- [7] Bally, J. 2016, *ARA&A*, 54, 491.
- [8] Blázquez-Calero, G. et al. 2023, in preparation
- [9] Chen, X., Arce, H. G., Zhang, Q., Launhardt, R., Henning, T. 2016, *ApJ*, 824, 72.
- [10] Masson, C. R., Chernin, L. M. 1993, *ApJ*, 414, 230.
- [11] Diaz-Rodriguez, A. K., Anglada, G., Blázquez-Calero, G. et al. 2022, *ApJ*, 930, 91.
- [12] Frank, A., Ray, T. P., Cabrit, S. et al. 2014, *prpl.conf*, 451.
- [13] Hatchell, J., Fuller, G. A., Ladd, E. F. 1999, *A&A*, 346, 278.
- [14] Hirano, N., Ho, P. P. T., Liu, S.-Y. et al. 2010, *ApJ*, 717, 58.
- [15] Hodapp, K. W., Chini, R. 2014, *ApJ*, 794, 169.
- [16] Lada, C. J. 1985, *ARA&A*, 23, 267.
- [17] Lee, C.-F., Hsu, M.-C., Sahai, R. 2009, *ApJ*, 696, 1630.
- [18] Lee, C.-F. 2020, *A&ARv*, 28, 1.
- [19] Lefloch, B., Cernicharo, J., Reipurth, B., Pardo, J. R., Neri, R. 2007, *ApJ*, 658, 498.
- [20] Plunkett, A. L., Arce, H. G., Corder, S. A., et al. 2013, *ApJ*, 774, 22.
- [21] Ray, T. P., Ferreira, J. 2021, *NewAR*, 93, 101615.
- [22] Rodríguez, L. F., Carral, P., Ho, P. T. P., Moran, J. M. 1982, *ApJ*, 260, 635.
- [23] Santiago-García, J., Tafalla, M., Johnstone, D., Bachiller, R. 2009, *A&A*, 495, 169.
- [24] Stephens, I. W., Dunham, M. M., Myers, P. C. et al. 2017, *ApJ*, 846, 16.
- [25] de A. Schutzer, A., Rivera-Ortiz, P. R., Lefloch, B. et al. 2022, *A&A*, 662, A104.
- [26] Tabone, B., Raga, A., Cabrit, S., Pineau des Forêts, G. 2018, *A&A*, 614, A119.
- [27] Tafalla, M., Su, Y.-N., Shang, H., et al., 2017, *A&A*, 597, A119.
- [28] Tychoniec, L., Hull, C. L. H., Kristensen, L. E. et al. 2019, *A&A*, 632, A101.